Subdiffraction-Limited Milling by an Optically Driven Single Gold Nanoparticle

Michael Fedoruk, Andrey A. Lutich,* and Jochen Feldmann*

Photonics and Optoelectronics Group, Physics Department and CeNS, Ludwig-Maximilians-Universität München, Amalienstr. 54, 80799 Munich, Germany

ABSTRACT We propose and demonstrate a hybrid lithographic technique capable of nanopatterning surfaces by optothermal decomposition of a polymeric film induced by a single metal nanoparticle. A tightly focused laser beam exerting a strong optical force onto the nanoparticle is used to move it inside the polymer film. Due to efficient plasmonic absorption of the laser light, the nanoparticle is heated up to temperatures of several hundred degrees, causing melting or even thermal decomposition of the polymer film. By this method, grooves less than 100 nm wide and tens of micrometers long can be directly milled in a polymer layer.

KEYWORDS: nanofabrication · metal nanoparticle · optical forces · plasmonic heating · thermal decomposition

There is an increasing demand for technologies capable of patterning surfaces at the nanoscale with high precision, high throughput, and in a cost-effective manner. For many applications, the desired patterning accuracy can be achieved using electron-beam[1,2] and ion-beam[3,4] lithography or scanning-probe methods[5] based on scanning tunneling microscopy[6] and/or atomic force microscopy[7] techniques. The simplest and most straightforward scanning-probe methods are based on mechanical scratching, etching, and removal of material *via* direct physical contact of the probe with the processed surface. For example, positioning the probe at specific surface locations and then applying a large force to the probe may result in irreversible indenting of the surface, which can be used to record structures.[7,8] The probe pressed against the substrate can then be scanned to produce lines. This technique is known as nanoshaving,[9] nanografting,[10] or plowing lithography.[11] The probe can be resistively heated to minimize the force needed to perform these types of lithographies on polymer surfaces.[12,13] Alternatively, the probe in close contact with the substrate is exposed to femtosecond laser pulses resulting in a tip-enhanced ablation.[14] Although the scanning methods result in the desired patterning accuracy, they are not suitable for large-scale production due to their serial essence, limiting the patterning throughput. The production of nanostructures by optical methods could enable the required high-speed patterning due to possible parallelization of light-based techniques. Due to the diffraction limit, however, the resolution of optical methods is limited to some hundreds of nanometers for visible light. Ideally, one would like to combine the advantages of both approaches utilizing the high accuracy of scanning-probe techniques and the ease of parallelization of optical methods.

In this article, we realize this idea by introducing a novel concept of an *optically driven nanoburner*. The nanoburner is a metal nanoparticle that is heated up due to strong plasmonic absorption of a focused laser beam and manipulated laterally due to optical forces exerted on it by the same laser beam. The heat released by the movable nanoparticle is used to perform thermally assisted milling in a polymer layer.

To demonstrate this method, we use spherical citrate-stabilized gold nanoparticles with diameters of 80 and 40 nm purchased from BBInternational. This type of metal nanoparticle has been extensively used for various applications due to its plasmon resonance, which lies in the optical spectral range. A polymer film with gold nanoparticles distributed homogeneously through the sample area is spin-coated on a glass slide and mounted on the scanning stage of an optical microscope equipped with dark-field illumination, enabling imaging and spectroscopy of single gold nanoparticles (Figure 1a). The optical microscope is adapted to include a laser beam that is focused slightly above the sample surface and thereby heats up and exerts optical forces on the nanoparticles within the polymer layer (Figure 1b).

* Address correspondence to andrey.lutich@physik.lmu.de, feldmann@lmu.de.

Received for review June 22, 2011 and accepted August 3, 2011.

Published online August 03, 2011
10.1021/nn2023045

© 2011 American Chemical Society

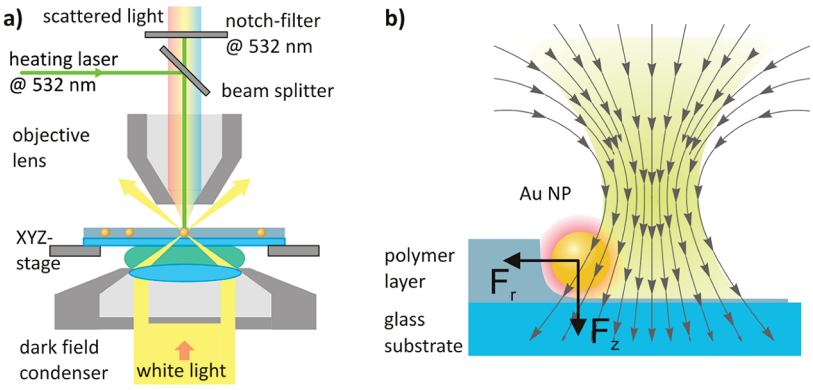

Figure 1. Optically driven golden nanoburner. (a) Diagram of the experimental setup. (b) Schematic representation of the optical forces acting on a nanoparticle inside a polymer layer during the patterning process. The laser beam is focused slightly above the substrate to utilize the radial optical force component of a divergent laser beam.

Since the pioneering work by Ashkin and coworkers,[15] the optical forces exerted by a tightly focused laser beam on micro- and nanoparticles have been widely used for micromanipulation purposes in biology, physics, chemistry, and material sciences.[16,17] Significant attention has been attracted by the problem of optical manipulation of metal nanoparticles[18−25] due to their unique plasmonic properties relevant to numerous important applications. The manipulation can be realized in two different ways: the nanoparticles can either be trapped at wavelengths red-shifted from their plasmon resonance and then moved to a point of interest[22,25,26] or they can be pushed along the beam propagation direction to a target position when using wavelengths resonant with the plasmon.[24,27−29] We have recently used the latter method to deposit single gold nanoparticles from a colloidal suspension onto a substrate with an accuracy of 50 nm[24] and to inject metal nanoparticles through phospholipid membranes into giant unilamellar vesicles.[29] In this study, we again do not use optical trapping to manipulate nanoparticles. Instead, we make use of the strong radial component of the optical pressure force present in a focused laser beam close to its focal plane (Figure 1b). This radial force is used to move the gold nanoparticles laterally in the sample plane. The use of a manipulating laser with the wavelength resonant (532 nm) with the plasmon of spherical gold nanoparticles has a two-fold effect. First, due to the enhanced interaction of metal nanoparticles with light at resonant wavelengths, the manipulation of nanoparticles is possible at lower laser powers. Second, the nanoparticles illuminated at their plasmon resonance can be heated up to several hundred degrees using moderate laser power densities,[25,30] which is necessary to realize a nanoburner capable of performing thermal patterning at the nanoscale.

Figure 2 illustrates the central result of this study: nanochannels milled in a PVA layer using the optically driven nanoburner. These channels were created by guiding gold nanoparticles laterally inside the PVA layer with the laser beam. Due to plasmonic heating, the nanoparticle is heated up to several hundred degrees (estimate for an 80 nm Au nanoparticle in PVA is >700 °C). This favors rapid melting (228 °C)[31] and thermal decomposition (520 °C)[32] of PVA molecules surrounding the nanoparticle and results in a groove left behind the nanoparticle as it is moved laterally. To support the thermal decomposition hypothesis, we have analyzed atomic force microscopy images of these grooves. We could not find any signature of the PVA being pressed out by the nanoparticle (Figure 2c).

The all-optical milling described here requires an appropriate combination of the axial and radial components of the optical force and the amount of heat absorbed/released by the nanoparticle. The ratio between the radial and axial components has to be maximized, and the amount of absorbed optical power has to be sufficient to decompose the polymer. Experimentally, for our material system, we have found that these conditions are fulfilled by placing the nanoparticle ~400 nm below the focal plane of the microscope objective (Figure 1b). We emphasize that the nanoparticle is not optically trapped but pushed in front of the defocused laser beam. Due to this defocusing, the beam diameter is enlarged in the particle's plane, resulting in an improved particle manipulation control.

The width of the channels itself can be adjusted by tuning the nanoparticle size used for the patterning. The nanochannel produced using a 40 nm gold nanoparticle is more than 10 μm long and only 49 nm wide, which is well below the diffraction limit for the wavelength of 532 nm used to manipulate the nanoparticle. Metal nanostructures are known to improve optical resolution beyond the diffraction limit by using electromagnetic field enhancement in nanogaps and at sharp tips. Here, we have demonstrated that the highly localized heating by metal nanoparticles is a promising opportunity to beat the diffraction limit. Although in our proof-of-concept experiment we have achieved the desired sub-100 nm feature size patterning of the PVA layer, the

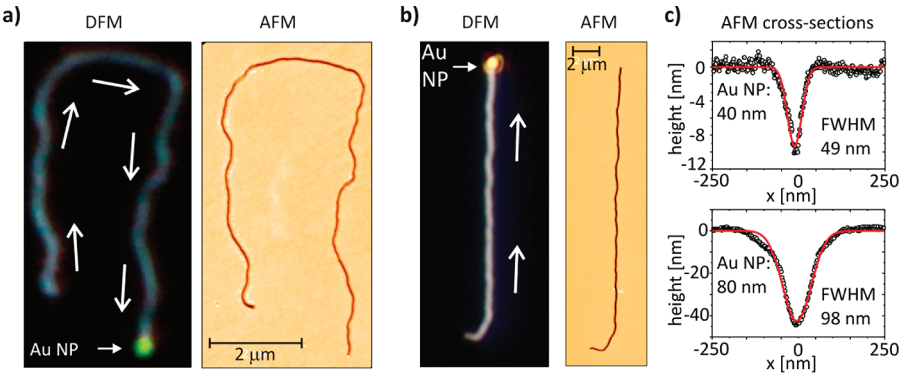

Figure 2. Subdiffraction-limited milling by a nanoburner. Nanochannels milled in a PVA layer by a single optically driven gold nanoparticle of (a) 40 nm and (b) 80 nm diameter. Both dark-field microscopy (left) and atomic force microscopy (right) images are present. The white arrows on the dark-field images indicate the direction of nanoparticle movement. In both cases, the nanoparticles were moved at an average speed of 5 μm/s. The nanoparticle is seen as a bright green (40 nm) or yellowish (80 nm) spot at the end of the channels. (c) Channels produced with nanoparticles of different sizes have different widths: a nanoparticle 40 nm large leads to a channel 49 nm wide (fwhm); (b) an 80 nm nanoparticle produces channels 98 nm wide (fwhm). The channels are all longer than 10 μm. The PVA layer thickness is ~35 nm and ~70 nm in the experiments with 40 and 80 nm diameter nanoparticles, respectively.

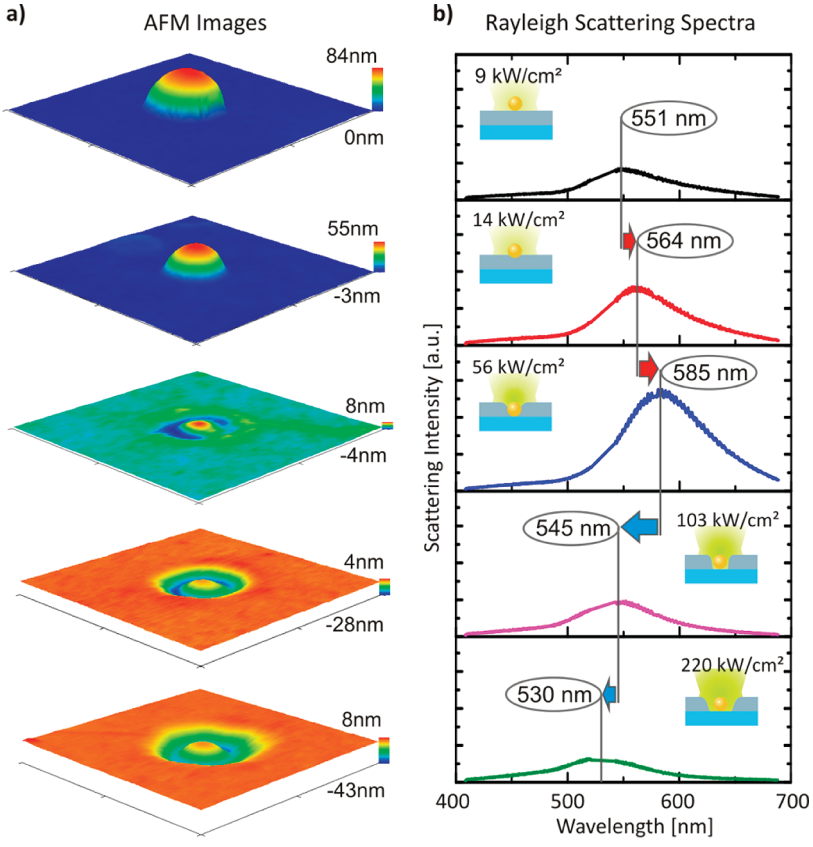

Figure 3. Laser embedding of gold nanoparticles into a polymer layer. (a) AFM images clearly show sinking of an 80 nm gold nanoparticle into the polystyrene layer upon plasmonic heating at lower laser powers and crater formation around the nanoparticle due to the thermal decomposition of the polystyrene at higher laser powers. (b) Rayleigh scattering spectra show an increasing refractive index around the nanoparticle seen as a red shifting and strengthening of the gold nanoparticle scattering. This shows how the embedding process occurs at moderate laser powers. The crater formation results in a blue shift of the spectra, which occurs due to a decrease of the refractive index around the nanoparticle. The laser power densities and corresponding scattering maxima are shown in panel (b).

guiding of nanoparticles in the polymer layer has to be improved in order to enable large arbitrarily shaped patterns with a high long-range accuracy.

The key issue in setting up controllable optical manipulation is an understanding of the optical forces acting on a metal nanoparticle during the writing

process. Here we recall that the optical forces pushing the nanoparticle are strongly dependent on the spectral position of the surface plasmon resonance with respect to the wavelength of the manipulating laser. The surface plasmon energy of metal nanoparticles is known to depend on the medium refractive index, which changes during the writing process due to the thermal decomposition of the surrounding PVA molecules. To assess this effect we drop-cast 80 nm gold nanoparticles from an aqueous solution onto an 80 nm thick polystyrene layer. Several individual nanoparticles were illuminated by a 532 nm laser at different laser powers. After illumination, atomic force microscopy imaging of nanoparticles exposed to different powers was performed (Figure 3a). In another experiment, we illuminated a single nanoparticle and the laser power was increased stepwise. After each illumination step, Rayleigh dark-field scattering spectroscopy was performed (Figure 3b).

As demonstrated in the experiment illustrated in Figure 3, the scattering cross section of a gold nanoparticle being used as a nanoburner for optothermal writing on a polymer layer may change considerably during this process. Upon thermally induced sinking of the nanoparticle into the polymer layer, the medium refractive index around the nanoparticle increases, causing, in turn, a red shift of the scattering spectrum. This optothermally assisted embedding of nanoparticles in a polymer film occurs at moderate laser power densities (<100 kW/cm^2 at 532 nm for 80 nm gold nanoparticles), and it has been recently proposed as a promising technology for high-density data storage devices.[33] Upon melting the polymer film and embedding a nanoparticle, a characteristic rim is formed around the nanoparticle formed by the polymer pressed out. At higher laser power densities, the plasmonic heating of the nanoparticle results in high temperatures favoring thermal decomposition of the polymer molecules around the nanoparticle. This decreases the medium refractive index seen by the nanoparticle and therefore leads to a blue shift of the scattering spectrum. At even higher laser power densities (>200 kW/cm^2 at 532 nm for 80 nm gold nanoparticles), the scattering spectrum shifts to the wavelengths even smaller than its initial position. This we attribute to the thermal decomposition of also surface ligands initially surrounding the nanoparticle. The optical pressure force used here to manipulate nanoparticles is directly proportional to the sum of absorption and scattering cross sections and, therefore, it also changes upon embedding of the nanoparticle in the polymer layer. The effect of the changing nanoparticle environment during the patterning process on the optical forces is influenced by a number of factors, including the laser wavelength, position of the nanoparticle with respect to the focal plane, and the actual effective refractive index around the

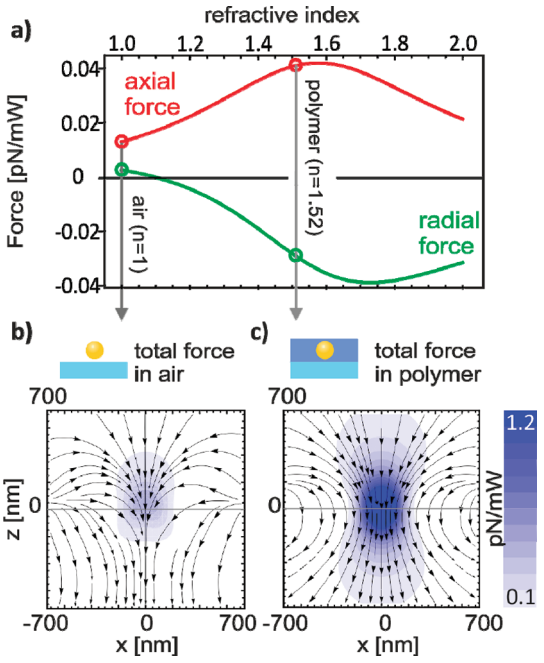

Figure 4. Lateral optical force depends strongly on the medium refractive index. (a) Axial (along beam axis, F_z) and the radial (along beam radius, F_r) optical forces have been calculated for different media refractive indices. An 80 nm gold nanoparticle has been placed 400 nm below the focal plane in the laser beam (532 nm) propagation direction and 400 nm away from the beam axis. A positive radial force points toward the beam axis, negative – outward. The map of the total optical force exerted in the proximity of the beam waist on an 80 nm gold nanoparticle in (b) air (n = 1) and (c) in a polymer-like medium (n = 1.52). The forces are calculated in units of pN per 1 mW of total beam power focused to a spot by an objective lens with NA = 0.9. For reference, the refractive indices of the glass, PVA, and polystyrene are 1.46, 1.52, and 1.55, respectively.

nanoparticle. To account for all of these parameters, we have carried out simulations of the optical forces in the paraxial beam approximation using scattering/gradient force formalism derived elsewhere.[34] Figure 4 illustrates the dependence of the optical forces on the medium refractive index.

The magnitude of the axial component (along beam axis) of the total optical force decreases more than two-fold upon reduction of the refractive index from 1.52, which corresponds to a polymer surrounding, to 1.0, corresponding to air. This effect is noticeable but not crucial because the drop of the force due to refractive index change can easily be compensated by increasing the laser power. In contrast to the axial force, the radial force, which is used to push nanoparticles inside the polymer layer, not only changes its magnitude but also its direction. In fact, the radial force becomes zero when the medium refractive index equals ~1.1. At higher refractive indices, the radial force is negative, that is, points outward from the beam axis enabling nanoparticles to be pushed in front of the laser beam. At refractive indices lower than 1.1, the radial force points toward

the beam axis excluding the possibility to push nanoparticles as depicted in Figure 1b. Total optical force maps calculated for different surroundings of an 80 nm nanoparticle in the proximity of the beam waist are presented in panels b and c of Figure 4. Comparing these panels, we conclude that the outwardly directed radial force present in polymer (n = 1.52) is not achievable in air (n = 1). This conclusion is also supported by experimental observations. First, it is not possible to move gold nanoparticles placed in air on a glass substrate or on a polymer film. To overcome this difficulty, nanoparticles in our patterning experiments were included into a polymer layer during the layer spin-coating step. Second, at high laser powers, the fast polymer decomposition around a nanoparticle prohibits moving the nanoparticles over long distances.

In conclusion, we have introduced a novel concept of optical milling of polymer films with sub-100 nm accuracy. This method uses a plasmonically heated single gold nanoparticle to record patterns by localized thermal decomposition of a polymer layer. The nanoparticle is plasmonically heated and moved laterally due to optical forces by a single focused laser beam. Highly localized heating by metal nanoparticles has been used for the first time to overcome the diffraction limit and record nanochannels with cross sections of 50 nm. The method is all-optical and, therefore, it can be easily parallelized using, for example, an acousto-optical deflector or a spatial light modulator.

METHODS

Experimental Setup. A Zeiss Axiotech 100 upright microscope equipped with dark-field illumination *via* an oil immersion condenser (Zeiss, NA 1.2−1.4) is adapted to include the manipulation laser (Millenia Vs 532 nm, Spectra-Physics). An air objective (Epiplan, Zeiss, 100×, NA 0.9) is used to simultaneously collect scattered light and focus the manipulation laser onto the sample. The sample position is controlled with piezo-driven stepper motor translation stages (Linos). Images are acquired using a digital camera (Canon EOS 550D). Scattering spectra are acquired using a spectrometer (Andor SpectraPro-300i) equipped with a CCD camera (Roper Scientific 1340/400).

Sample Preparation. Spherical citrate-stabilized gold nanoparticles with diameters of 80 and 40 nm were purchased from BBInternational and used without additional purification. The colloidal nanoparticle solution is mixed with a polyvinyl alcohol (PVA) solution and spin-coated on a glass substrate, resulting in a polymer film with gold nanoparticles distributed homogeneously through the polymer film with a particle surface density of 5×10^4 to 6×10^5 cm^{-2}. The particle density is estimated by counting a number of particles on a dark-field image within a 50×50 μm square.

Simulations. COMSOL Multiphysics 4.0 finite-element calculations were performed to estimate steady-state temperatures raised by absorption of the manipulating laser light. Optical forces exerted by light onto gold nanoparticles were calculated in the paraxial beam approximation using scattering/gradient force formalism derived elsewhere.[34] These simulations were implemented in Wolfram Mathematica 8.0.

Acknowledgment. We are thankful to our colleagues A. Ohlinger and A. Urban for reading the manuscript and their helpful comments. Financial support by the DFG through the Nanosystems Initiative Munich (NIM) by the ERC through the Advanced Investigator Grant HYMEM is gratefully acknowledged.

REFERENCES AND NOTES

1. Nakayama, Y. Electron-Beam Cell Projection Lithography: A New High-Throughput Electron-Beam Direct-Writing Technology Using a Specially Tailored Si Aperture. *J. Vac. Sci. Technol., B* **1990**, *8*, 1836.
2. Pain, L.; Icard, B.; Manakli, S.; Todeschini, J.; Minghetti, B.; Wang, V.; Henry, D. Transitioning of Direct e-Beam Write Technology from Research and Development into Production Flow. *Microelectron. Eng.* **2006**, *83*, 749–753.
3. Ximen, H. Focused Ion Beam Micromachined Three-Dimensional Features by Means of a Digital Scan. *J. Vac. Sci. Technol., B* **1990**, *8*, 1361.
4. Chason, E.; Picraux, S. T.; Poate, J. M.; Borland, J. O.; Current, M. I.; Diaz de la Rubia, T.; Eaglesham, D. J.; Holland, O. W.; Law, M. E.; Magee, C. W.; *et al.* Ion Beams in Silicon Processing and Characterization. *J. Appl. Phys.* **1997**, *81*, 6513.
5. Saavedra, H. M.; Mullen, T. J.; Zhang, P.; Dewey, D. C.; Claridge, S. A.; Weiss, P. S. Hybrid Strategies in Nanolithography. *Rep. Prog. Phys.* **2010**, *73*, 036501.
6. Kleineberg, U.; Brechling, A.; Sundermann, M.; Heinzmann, U. STM Lithography in an Organic Self-Assembled Monolayer. *Adv. Funct. Mater.* **2001**, *11*, 208–212.
7. Vanlandingham, M. R.; McKnight, S. H.; Palmese, G. R.; Elings, J. R.; Huang, X.; Bogetti, T. A.; Eduljee, R. F.; Gillespie, J. W. Nanoscale Indentation of Polymer Systems Using the Atomic Force Microscope. *J. Adhes.* **1997**, *64*, 31–59.
8. Sirghi, L.; Ruiz, A.; Colpo, P.; Rossi, F. Atomic Force Microscopy Indentation of Fluorocarbon Thin Films Fabricated by Plasma Enhanced Chemical Deposition at Low Radio Frequency Power. *Thin Solid Films* **2009**, *517*, 3310–3314.
9. Chwang, A. B.; Granstrom, E. L.; Frisbie, C. D. Fabrication of a Sexithiophene Semiconducting Wire: Nanoshaving with an Atomic Force Microscope Tip. *Adv. Mater.* **2000**, *12*, 285–288.
10. Xu, S.; Miller, S.; Laibinis, P. E.; Liu, G.-yu Fabrication of Nanometer Scale Patterns within Self-Assembled Monolayers by Nanografting. *Langmuir* **1999**, *15*, 7244–7251.
11. Cappella, B. Breaking Polymer Chains by Dynamic Plowing Lithography. *Polymer* **2002**, *43*, 4461–4466.
12. Mamin, H. J.; Rugar, D. Thermomechanical Writing with an Atomic Force Microscope Tip. *Appl. Phys. Lett.* **1992**, *61*, 1003.
13. Vettiger, P.; Brugger, J.; Despont, M.; Drechsler, U.; Durig, U.; Haberle, W.; Lutwyche, M.; Rothuizen, H.; Stutz, R.; Widmer, R. Ultrahigh Density, High-Data-Rate NEMS-Based AFM Data Storage System. *Microelectron. Eng.* **1999**, *46*, 11–17.
14. Chimmalgi, A.; Grigoropoulos, C. P.; Komvopoulos, K. Surface Nanostructuring by Nano-/Femtosecond Laser-Assisted Scanning Force Microscopy. *J. Appl. Phys.* **2005**, *97*, 104319.
15. Ashkin, A.; Dziedzic, J. M.; Bjorkholm, J. E.; Chu, S. Observation of a Single-Beam Gradient Force Optical Trap for Dielectric Particles. *Opt. Lett.* **1986**, *11*, 288–290.
16. Dienerowitz, M.; Mazilu, M.; Dholakia, K. Optical Manipulation of Nanoparticles: A Review. *J. Nanophotonics* **2008**, *2*, 021875-32.
17. Jonas, A.; Zemánek, P. Light at Work: The Use of Optical Forces for Particle Manipulation, Sorting, and Analysis. *Electrophoresis* **2008**, *29*, 4813–4851.
18. Svoboda, K.; Block, S. M. Optical Trapping of Metallic Rayleigh Particles. *Opt. Lett.* **1994**, *19*, 930–932.

19. Hansen, P. M.; Bhatia, V. K.; Harrit, N.; Oddershede, L. Expanding the Optical Trapping Range of Gold Nanoparticles. *Nano Lett.* **2005**, *5*, 1937–1942.
20. Bosanac, L.; Aabo, T.; Bendix, P. M.; Oddershede, L. B. Efficient Optical Trapping and Visualization of Silver Nanoparticles. *Nano Lett.* **2008**, *8*, 1486–1491.
21. Tong, L.; Miljković, V. D.; Johansson, P.; Käll, M. Plasmon Hybridization Reveals the Interaction between Individual Colloidal Gold Nanoparticles Confined in an Optical Potential Well. *Nano Lett.* **2011**, DOI: 10.1021/nl1036116.
22. Ito, S.; Yoshikawa, H.; Masuhara, H. Laser Manipulation and Fixation of Single Gold Nanoparticles in Solution at Room Temperature. *Appl. Phys. Lett.* **2002**, *80*, 482.
23. Yoshikawa, H.; Matsui, T.; Masuhara, H. Reversible Assembly of Gold Nanoparticles Confined in an Optical Microcage. *Phys. Rev. E* **2004**, 70.
24. Urban, A. S.; Lutich, A. A.; Stefani, F. D.; Feldmann, J. Laser Printing Single Gold Nanoparticles. *Nano Lett.* **2010**, *10*, 4794–4798.
25. Ohlinger, A.; Nedev, S.; Lutich, A. A.; Feldmann, J. Optothermal Escape of Plasmonically Coupled Silver Nanoparticles from a Three-Dimensional Optical Trap. *Nano Lett.* **2011**, *11*, 1770–1774.
26. Prikulis, J.; Svedberg, F.; Käll, M.; Enger, J.; Ramser, K.; Goksör, M.; Hanstorp, D. Optical Spectroscopy of Single Trapped Metal Nanoparticles in Solution. *Nano Lett.* **2004**, *4*, 115–118.
27. Ashkin, A. Acceleration and Trapping of Particles by Radiation Pressure. *Phys. Rev. Lett.* **1970**, *24*, 156–159.
28. McDougall, C.; Stevenson, D. J.; Brown, C. T. A.; Gunn-Moore, F.; Dholakia, K. Targeted Optical Injection of Gold Nanoparticles into Single Mammalian Cells. *J. Biophotonics* **2009**, *2*, 736–743.
29. Urban, A. S.; Pfeiffer, T.; Fedoruk, M.; Lutich, A. A.; Feldmann, J. Single Step Injection of Gold Nanoparticles through Phospholipid Membranes. *ACS Nano* **2011**, *5*, 3585–3590.
30. Stehr, J.; Hrelescu, C.; Sperling, R. A.; Raschke, G.; Wunderlich, M.; Nichtl, A.; Heindl, D.; Kurzinger, K.; Parak, W. J.; Klar, T. A.; Feldmann, J. Gold NanoStoves for Microsecond DNA Melting Analysis. *Nano Lett.* **2008**, *8*, 619–623.
31. Tubbs, R. K. Melting Point and Heat of Fusion of Poly(vinyl alcohol). *J. Polym. Sci. A* **1965**, *3*, 4181–4189.
32. Fernandes, D. M.; Hechenleitner, A. A. W.; Pineda, E. A. G. Kinetic Study of the Thermal Decomposition of Poly(vinyl alcohol)/Kraft Lignin Derivative Blends. *Thermochim. Acta* **2006**, *441*, 101–109.
33. Skirtach, A. G.; Kurth, D. G.; Mohwald, H. Laser-Embossing Nanoparticles into a Polymeric Film. *Appl. Phys. Lett.* **2009**, *94*, 093106-3.
34. Arias-González, J. R.; Nieto-Vesperinas, M. Optical Forces on Small Particles: Attractive and Repulsive Nature and Plasmon-Resonance Conditions. *J. Opt. Soc. Am. A* **2003**, *20*, 1201.